Heliyon 10 (2024) e34723

Contents lists available at ScienceDirect

Heliyon

journal homepage: www.cell.com/heliyon

Research article

A preliminary study on ultrasound techniques applied to evaluate the curative effect of botulinum toxin type a in hypertrophic scars

Liu-liu Cao [a,1], Zhi-guo Yang [b,1], Wei-hong Qi [a], Huan Zhang [a], Yu Bi [a], Yong Shan [a], Xin-wu Cui [c], Fan Jiang [a,*]

[a] Department of Medical Ultrasound, The Second Hospital of Anhui Medical University, Hefei, 230601, Anhui Province, China
[b] Department of Plastic and Reconstructive Surgery, The Second Hospital of Anhui Medical University, Hefei, 230601, Anhui Province, China
[c] Department of Medical Ultrasound, Tongji Hospital, Tongji Medical College, Huazhong University of Science and Technology, Wuhan Province, China

ARTICLE INFO

Keywords:
Botulinum toxin type A
Hypertrophic scar
High-frequency ultrasound
Superb microvascular imaging
Shear wave elastography

ABSTRACT

Objective: To validate the feasibility of ultrasound in assessing the curative effect of botulinum toxin type A (BTXA) in treating hypertrophic scar (HS).
Methods: Eight healthy New Zealand long-eared rabbits were utilized in the study. Four wounds, each measuring 1.0 cm in diameter, were created on both ears of each rabbit. Immediately after surgery, each of these wounds received an injection containing a distinct concentration of BTXA. On postoperative week 6, scar thickness, vascularity, and hardness were assessed based on high frequency ultrasound (HFUS), superb microvascular imaging (SMI), shear wave elastography (SWE), Masson staining, and immunohistochemical staining for CD31.
Results: All wounds healed well, and HSs formed after 6 weeks post-surgery. Scar thickness based on HFUS presented a significant decrease with increasing BTXA concentration ($p < 0.05$), aligning with the gross morphology. Simultaneously, scar stiffness, evaluated using SWE, showed a significant decrease in accordance with the variation of the collagen volume fraction, which refers to the ratio of the collagen positive area to the total area ($p < 0.05$). Although the vascularity index obtained by SMI did not exhibit a statistically significant change across different BTXA concentrations, this technique effectively illustrated the microvascular perfusion in HS. Immunohistochemical staining for CD31 revealed that BTXA inhibited angiogenesis.
Conclusion: HFUS and SWE displayed excellent performance in evaluating HS thickness and stiffness. SMI showed a good performance in reflecting microvascular signals in HS. These ultrasound techniques have great potential in assessing the therapeutic effect of BTXA in HS.

1. Introduction

Hypertrophic scar (HS) represents a type of pathological scar characterized by persistent hyperplasia in the scar tissue, which manifests during the dermal wound healing process [1]. The characteristics of HS are that it displays dermal fibroblast

* Corresponding author.
E-mail addresses: aydcll2016@163.com (L.-l. Cao), 1131392404@qq.com (Z.-g. Yang), 123qiweihong@163.com (W.-h. Qi), zhcherish@163.com (H. Zhang), aydby0311@163.com (Y. Bi), shanyongah@163.com (Y. Shan), cuixinwu@live.cn (X.-w. Cui), ahultrasound2005@126.com (F. Jiang).
[1] These two authors contributed equally to this work.

https://doi.org/10.1016/j.heliyon.2024.e34723
Received 21 May 2023; Received in revised form 12 July 2024; Accepted 15 July 2024
Available online 19 July 2024

hyperproliferation, collagen overproduction, and excess extracellular matrix deposition resulting from traumatic injuries, deep burns, and even acne [2]. It is reported that 17–67 % of patients with traumatic skin injuries and surgical procedures will develop HS on the skin [3–5]. HS could not only affect the skin's appearance and function but also result in psychological stress in millions of patients globally [6]. Patients with HSs have to suffer from pain, pruritus, and reduced quality of life [7].

Currently, there are a variety of HS treatments, including surgical and nonsurgical resection approaches, such as compression, silicone sheet, corticosteroid injection, cryotherapy, laser treatment, intralesional 5-FU injections, and intralesional botulinum toxin type A (BTXA) injections [8,9]. The utilization of corticosteroid injections is prevalent in the treatment of scars owing to its notable effectiveness [10]. Nevertheless, prolonged administration of corticosteroids may result in complications such as localized skin atrophy and capillary dilation, with an associated incidence rate reaching as high as 63 % [11]. Additionally, excessive dosages can precipitate systemic adverse reactions [12]. In recent years, intralesional BTXA injection has become one of the most promising approaches and increasing numbers of physicians prefer BTXA for HS treatment and prevention, due to its proven ability to inhibit scar formation and lack of significant side effects [13]. As is well established, HS primarily results from tension exerted on wound edges. BTXA is able to inhibit acetylcholine release into the neuromuscular junction, which could lead to muscle paralysis and consequently reduce wound tension [13]. Owing to this mechanism and others, BTXA can be applied not only for the treatment of HS but also for its prevention [13].

HS treatment varies depending on its developmental stage, and the occurrence of both over- and undertreatment is prevalent in clinical practice. Therefore, the assessment of HS at different stages holds significant importance in its effective management. As is widely recognized, pathological examination serves as the definitive method for diagnosing a variety of diseases; however, biopsies frequently pose a risk of infection, which can have a negative impact on wound healing outcomes [14]. Therefore, finding noninvasive and simple methods to evaluate HSs is required. With the rapid development of medical science, there are various subjective and objective methods used to evaluate scars. Subjective approaches are mainly applied in clinics, including the Vancouver Scar Scale (VSS), modified Seattle scale, and standardized questionnaire, which are totally clinician- and patient-dependent [15,16]. A large number of noninvasive tools are able to provide a more objective and accurate evaluation and monitoring of scars, including dermoscopy [17], laser speckle contrast imaging [18,19], and ultrasound. Although dermoscopy is able to visualize vascular structure, it is limited to displaying only the upper layer of tissue [17]. Laser speckle contrast imaging could monitor blood perfusion but without a good penetration depth [19]. In recent years, ultrasound has become widely used in dermatological research, involving gray-scale ultrasound, color doppler ultrasound, power doppler ultrasound, elastography, and microvessel blood flow imaging.

Conventional grayscale ultrasound could be employed for a more accurate determination of scar thickness, enabling the assessment of both scar height and penetration depth (depth below the surface). Ultrasounds above 20 MHz are considered high frequency ultrasound (HFUS) [20]. It has a better performance in assessing the thickness of small scars and has been generally used to assess skin echogenic changes [21]. It is reported that credible and accurate vascularity measurement could help monitor scar changes and adopt targeted interventions to prevent excessive scarring [22]. Color and power doppler were used to detect vascularity in scars [23], which had a poor performance in displaying micro-low-speed blood flow signals and could not be applied for quantitative analysis. By contrast, superb microvascular imaging (SMI), known as an emerging ultrasound technology, is able to separate low-speed blood flow signals from slow mixed clutter signals based on an adaptive algorithm, so as to display the micro-low-speed blood flow signals more clearly and completely. SMI has been applied to diagnose and assess the development of many human diseases, including tumors, injury, and inflammation among others [24]. It also has the ability to provide a vascularity index (VI) based on automated application, which could reflect the proportion of blood flow within the tissue. Therefore, SMI may have a better performance in assessing vascularity in HS. Elastography, particularly shear wave elastography (SWE), has been applied in many studies in assessing scar stiffness [21,25,26]. It can provide objective quantification of tissue stiffness by using multiple, rapid ultrasound images to capture shear-wave propagation away from the region of force excitation based on an ultrasound platform [25].

SMI and SWE have been used to evaluate cicatricial plaques in cicatricial alopecia patients and had a good performance in showing scar fibrosis and inflammation [27]. However, these two ultrasound techniques have not been specifically applied to scars in the clinic. Therefore, we preliminarily validated the effectiveness and credibility of these techniques in evaluating the therapeutic effects of BTXA in the early stage of HS formation with animal models. In this research, SMI was employed to evaluate scar vascular perfusion, SWE was utilized to assess scar stiffness, and HFUS was employed to measure scar thickness in order to compare the therapeutic efficacy of varying concentrations of BTXA on HS. Given that scars primarily consist of excess collagen in distinct nodules, resulting in heightened stiffness and reduced elasticity, the collagen content was quantified to validate the precision of SWE in assessing scar hardness [28]. In contrast to the wound contraction observed in rodents, skin wounds in rabbit ears predominantly heal through reepithelialization due to the strong adherence between the dermis and subcutaneous tissue layer, resulting in hypertrophic scarring similar to that seen in humans [29]. Therefore, a rabbit ear scar model was developed for the purposes of this study. Masson's staining was utilized to assess the collagen content of scar tissue through pathological examination in order to validate the efficacy of SWE in assessing scar hardness. Additionally, immunohistochemistry was employed to measure CD31 levels as a marker of angiogenesis, providing a more comprehensive evaluation of the accuracy of SMI technology. To the best of our knowledge, this is the first study to validate the performance of SMI in assessing therapeutic effects in HS treatment in the early stage of HS formation.

2. Materials and methods

This study was reviewed and approved by the Animal Experimentation Ethics Committee of Anhui Medical University (ethics number: LLSC20221114).

2.1. Materials

Animals. Eight healthy adult New Zealand long-eared rabbits were obtained from the Anhui Medical University Animal Test Center, weighing 2,000–3,000 g, both females and males, were involved in this study. All rabbits were housed by professional breeders in standard animal rooms at 23 °C ± 2 °C, 50%–60 % relative humidity, and >8 h/day of light, with free access to food and water.

2.2. Methods

2.2.1. Hypertrophic scar modeling

The experimental method of the animal model was developed based on our previous study [30]. The rabbits were anesthetized with sodium pentobarbital (30 mg/kg). The ventral sides of both ears were cleaned to fully expose the superficial vessels to avoid injury during the experiment. Four circular areas of 1.0 cm in diameter and at a 1.5 cm interval were marked on each side of the ventral midline of both ears using a circle gauge and methylene blue (Fig. 1). The ears were disinfected three times with iodine complex, the full skin was removed aseptically, and the perichondrium of each wound was removed under a light microscope to facilitate proliferative scar formation. Finally, the wound was re-sterilized and exposed for BTXA intervention after applying pressure with gauze to stop the bleeding.

2.2.2. BTXA intervention

After modeling, four wounds were obtained from both ears and were randomly divided in each ear into the 0 U/ml, 5 U/ml, 10 U/ml, and 20 U/ml groups, with a total of 16 wounds in each group. BTXA (Lanzhou Hengli, Lanzhou Biological Company) stored at −20 °C was placed at room temperature for 15–20 min and diluted with saline into different therapeutic concentration solutions for use. 0 U/ml group was injected with saline. After each rabbit ear was molded, 0.2 ml BTXA (0.05 ml each at 3, 6, 9, and 12 o'clock) was injected immediately outside the wound margin.

2.2.3. Postoperative observation and sampling

Following surgery, the general condition of the animals was closely observed, and the wound dressing was changed every other day. The wound healing and epithelialization time were dynamically observed and recorded. During the initial week, our observations were conducted every two days, followed by weekly observations thereafter. After the hypertrophic scar was formed and stabilized at 6 weeks postoperatively, we first assessed the scar proliferation using ultrasound, then euthanized the rabbits and took scar samples, including at least 5 mm of normal skin around the scar, which were immediately fixed in 10 % neutral formaldehyde for subsequent staining assessment.

Fig. 1. Four wounds were obtained after modeling.

2.2.4. Ultrasound evaluation

Prior to the assessment, the hair on both ears was removed with a mild and non-stimulating method. After waiting for 10 min, the pad filled with an ultrasonic gel was laid on the scar and the transducer was placed onto the pad. All scars were examined by high-frequency ultrasound using a musculoskeletal ultrasonic diagnostic system (Aplio i800, Canon, Japan). During the measurement process, it is important to maintain the orientation of the probe parallel to the long axis of the rabbit ear. The image was frozen at the thickest point of both the epidermis and dermis layers of the scar. The total thickness of these layers was measured, and the average value of three consecutive measurements were calculated. All examinations were performed with the same i24LX8 linear probe at the same frequency of 24 MHz, and thicknesses of all the scars at the thickest point were measured by the same physician (L C). Subsequently, on the basis of gray-scale image, the instrument was switched to the SMI mode and the speed scale was set at 1.2 cm/s. In the SMI model, a square of the same size was selected as the region of interest (ROI), with the scar positioned at the center of it. Subsequently, the VI, presented as the percentage form, was calculated automatically by the system. SWE examination was undertaken by the same experienced sonographer using the Siemens ACUSON Sequoia with a 10L4 linear probe operating at 3–10 MHz. The measurement range was set 0.5 m/s-10 m/s. We still maintained the orientation of the probe parallel to the long axis of the rabbit ear and activated SWE mode at the thickest part of the scar. Then we established the sampling frame, encompassing both the scars and the surrounding normal tissue. After acquiring a stable color-coded square frame, a circular ROI was placed at the scar to measure the shear wave velocity (Fig. 2). It was of great significance to ensure that there was no pressure between the probe and skin throughout the process. Moreover, in order to reduce the measurement error, every recording was repeated three times by the same experienced person, and the value was calculated by averaging these three measurements.

2.2.5. Immunohistochemical staining for CD31

For immunohistochemistry, following staining and incubation, the paraffin sections were sealed using neutral gum, and images were obtained. Image J software was used for image quantization analysis. The average optical density (AOD) was measured to reflect the concentration of the target protein per unit area. AOD = integrated optical density/positive area.

2.2.6. Masson's trichrome staining and collagen volume fraction (CVF) measurement

Following the ultrasound evaluation, Masson staining was performed using the Masson staining kit (cat. B022, ebiogo). Following staining, the sections were placed under a microscope (OLYMPUS CX41) to observe the collagen proliferation of each group of scars. Quantitative analysis was normally performed by calculating the CVF using Image J software. Five fields of view were randomly

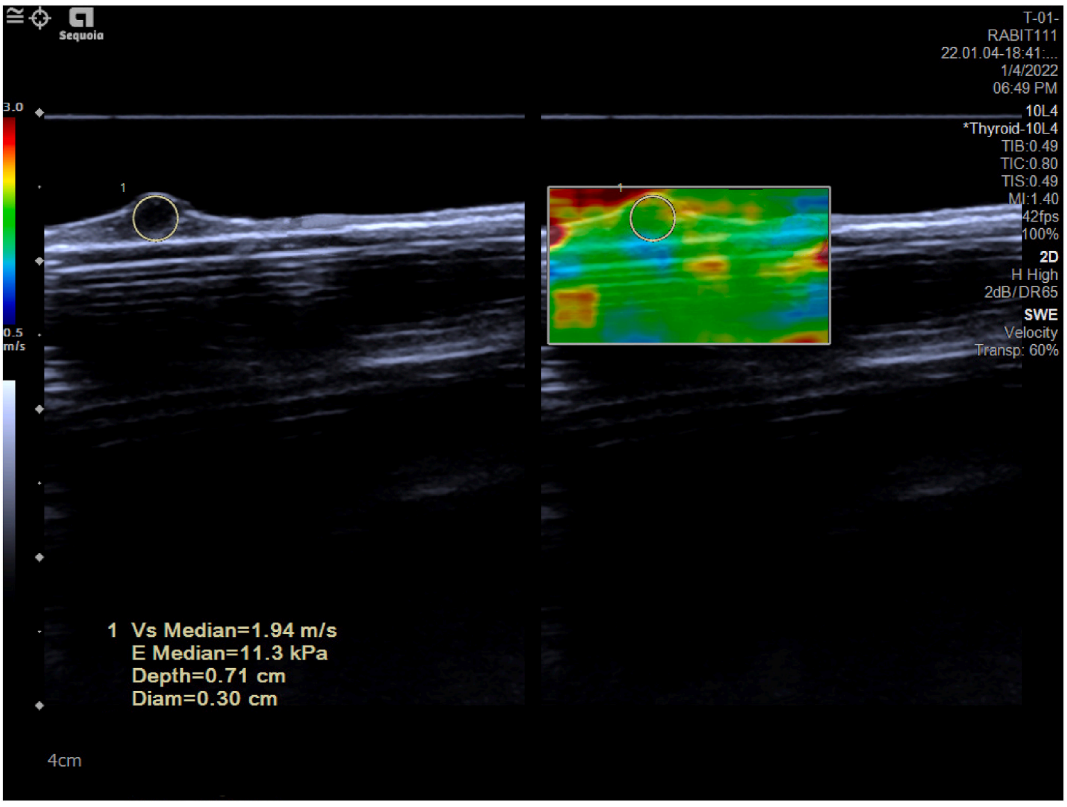

Fig. 2. Shear wave elastography images of hypertrophic scars. The median values of shear wave velocity and Young's modulus were automatically displayed on the image. The square on the right of the picture represents the sampling frame, and the circle represents the region of interest.

selected under a light microscope at 200 × magnification, and the average CVF of the five fields of view was taken as the final result. CVF = (collagen positive area/total area) × 100 %.

2.2.7. Statistical analysis

The quantitative data were presented as mean ± standard deviation. Statistical analyses were performed using one-way analysis of variance with SPSS software 25.0. Bonferroni test was used for post hoc multiple comparisons, and $p < 0.05$ was considered to demonstrate statistical significance.

3. Results

3.1. Changes of wounds and general observation of HSs

In our study, all wounds healed well. As shown in Fig. 3, local protuberance on the wound surface 12 days after operation was a sign of HS formation. Six weeks after surgery, the wound healed completely and a bulge appeared in the center of the scar, but the bulge did not extend beyond the edge of the scar.

3.2. Thickness evaluation of HSs based on high frequency ultrasound on treatment with different BTXA concentrations

The total thicknesses of both epidermis and dermis layers of the scar in different groups were measured (Fig. 4a). The mean thicknesses of the groups were 4.25 ± 0.12 mm, 3.87 ± 0.14 mm, 3.41 ± 0.12 mm, and 2.59 ± 0.13 mm in the 0 U/ml, 5 U/ml, 10 U/ml, and 20 U/ml groups, respectively (Fig. 4b). Differences between groups were statistically significant after post hoc multiple comparisons ($p < 0.05$).

3.3. HS evaluation based on SMI on treatment with different BTXA concentrations

The VI obtained by SMI could reflect the microvessel density (Fig. 5). However, in the present study, there was no significant difference between all groups ($p > 0.05$).

3.4. HS evaluation based on SWE on treatment with different BTXA concentrations

The values of shear wave velocity of different groups were measured (Fig. 6a). The mean values of the shear wave velocity of the groups were 3.31 ± 0.32 m/s, 2.72 ± 0.25 m/s, 2.10 ± 0.28 m/s, and 1.55 ± 0.15 m/s in the 0 U/ml, 5 U/ml, 10 U/ml, and 20 U/ml groups, respectively (Fig. 6b). There was statistical significance between groups after post hoc multiple comparisons ($p < 0.05$).

3.5. Evaluation of HS angiogenesis based on CD31 staining

Images of immunohistochemical staining for CD31 in the different groups were displayed in Fig. 7a. The mean AOD values of different groups were 0.52 ± 0.04, 0.49 ± 0.03, 0.38 ± 0.03, and 0.17 ± 0.04 in the 0 U/ml, 5 U/ml, 10 U/ml, and 20 U/ml groups, respectively (Fig. 7b). Differences between groups were statistically significant after post hoc multiple comparisons ($p < 0.05$).

3.6. BTXA inhibited collagen proliferation with increasing concentration

Images of Masson staining in the different groups were displayed in Fig. 8a. The mean values of the CVF (%) of the groups were 76.38 ± 2.03, 68.77 ± 2.28, 56.58 ± 1.86, and 45.83 ± 1.90 in the 0 U/ml, 5 U/ml, 10 U/ml, and 20 U/ml groups, respectively (Fig. 8b). Differences between groups had statistical significance after posterior comparisons ($p < 0.05$).

Fig. 3. Changes of hypertrophic scar in rabbit ears.

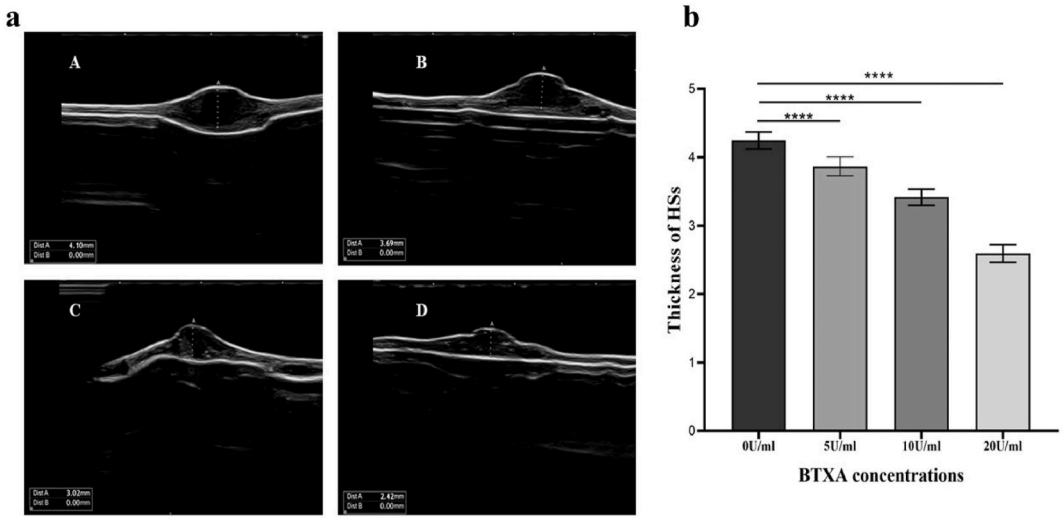

Fig. 4. High-frequency ultrasound results of the different groups. a Hypertrophic scar thickness in the 0 U/ml (A), 5 U/ml (B), 10 U/ml (C), and 20 U/ml (D) groups. b Hypertrophic scar thickness in the different groups. Compared with the 0 U/ml group, all differences were statistically significant (****$p < 0.001$).

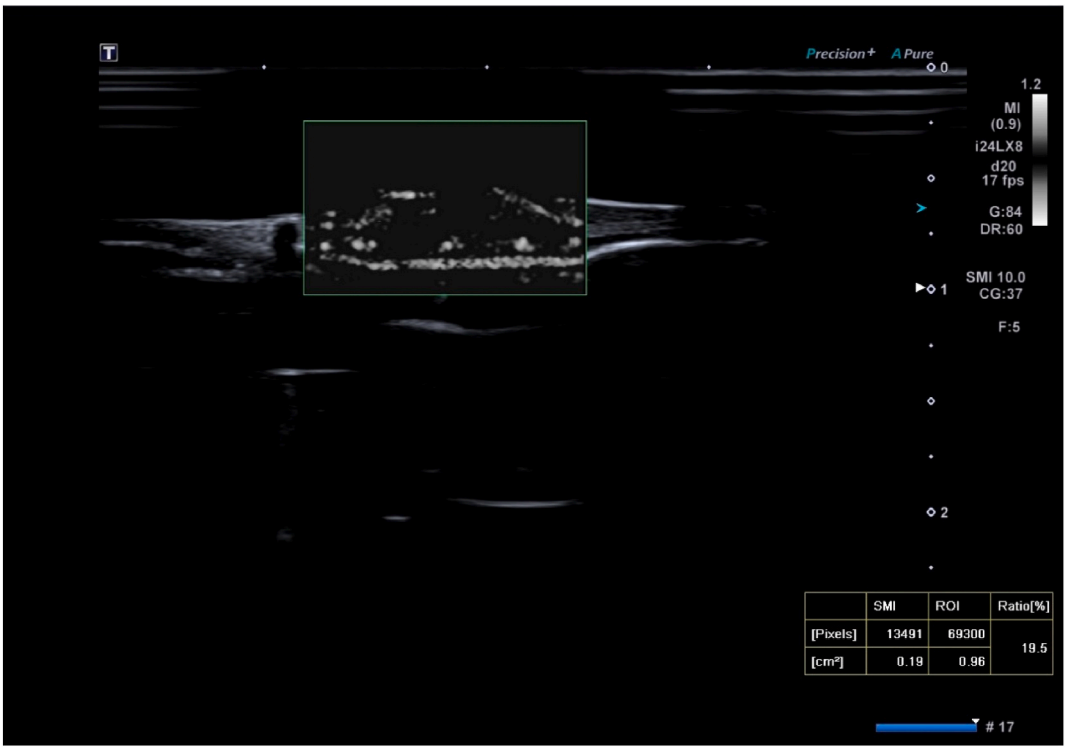

Fig. 5. Scar vascularity is shown and the vascularity index was calculated automatically based on superb microvascular imaging. The blood flow signal can be seen in the superb microvascular imaging as a bright white area.

4. Discussion

By using rabbit ear scar models, our experiment evaluated the performance of ultrasound in assessing the curative effect of BTXA in treating scars. We observed a decrease in both scar thickness and shear wave velocity of scars with an increase in treatment concentration ($p < 0.05$), consistent with the general observation and pathological results. SMI could clearly display the microvascular perfusion in the scar.

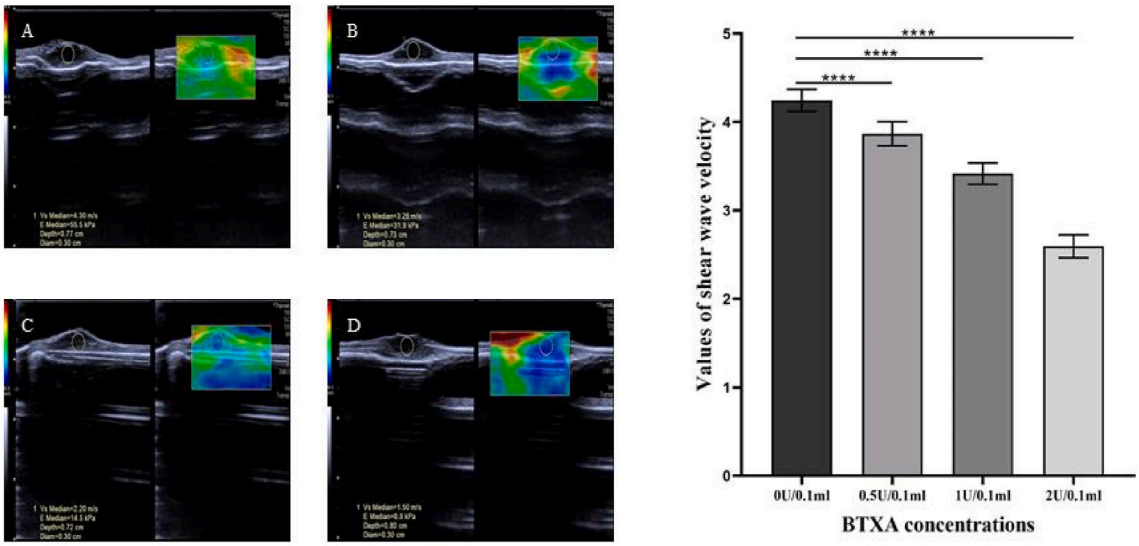

Fig. 6. Shear wave elastography results of different groups. a Shear wave elastography images of HSs after measurement in the 0 U/ml (A), 5 U/ml (B), 10 U/ml (C), and 20 U/ml (D) groups. b The mean values of the scar shear wave velocity in the different groups. Compared with the 0 U/ml group, all differences were statistically significant ($^{****}p < 0.001$).

HS evaluation is important for assessing therapeutic effects, which would be of benefit in guiding further treatment and promoting HS prognosis. Therefore, finding noninvasive methods that could provide a reliable HS evaluation is significant. Ultrasound is one of the first-line examination techniques in clinical settings, which could provide noninvasive high-resolution imaging of skin and subcutaneous tissues. In recent years, rapidly developing ultrasound techniques, including SWE and SMI, have shown promise in offering more comprehensive information about scars. To the best of our knowledge, this study represents the first attempt to validate the performance of these techniques in assessing the therapeutic effects of HS treatment in the early stages of HS formation. Moreover, scars were examined histologically in this study, enhancing the objectivity of evaluating the accuracy of the ultrasound.

Scar thickness is an important component of scar evaluation. However, existing methods for evaluating scar tissue thickness have some limitations. For example, VSS is subjective, resulting in high variabilities in evaluation. Moreover, its hierarchical assessment method may not be sensitive enough when minor changes in scar thickness occur. For example, when scar thickness is reduced from 5 mm to 3 mm, the score may remain unchanged. By contrast, HFUS is more sensitive to subtle changes. A previous study, which compared scar thickness before and after treatment in 22 patients using HFUS, showed a more significant improvement in scar thickness after treatment compared with VSS [23]. This confirmed the high sensitivity of HFUS in the assessment of scar thickness. Although histological evaluation via biopsy could display different layers of normal skin and scars, such a method is invasive and not practical for clinical application. As a noninvasive and objective approach capable of creating valid and reproducible results in scarred tissue, HFUS has been recommended in recent studies for the assessment of scar thickness [31].

In our study, scar thickness significantly decreased with increasing BTXA concentration, which was in accordance with the general scar observations. Moreover, this method presented good consistency throughout our measurements. In future clinical work, HFUS could be employed to assess scar thickness to evaluate therapeutic effects.

Vascularity is a significant parameter associated closely with scar maturation [32,33], and several earlier studies demonstrated that BTXA could inhibit angiogenesis [34]. Therefore, we evaluated the therapeutic effect of BTXA by assessing vascularity. In a previous study, researchers attempted to construct three-dimensional images of blood vessels in the HS to clarify the vascular patterns based on pathological and histological examinations [35]. However, using this invasive evaluation tool in clinics is unrealistic. Additionally, numerous subjective vascularity measurement scales are used to evaluate vascularity, offering only a preliminary and subjective impression of scar vascularity [23]. In contrast to measurement scales, ultrasound is more objective and has been increasingly used for noninvasive vascularity evaluation. Previous studies, for instance, utilized color Doppler and power Doppler for scar vascularity evaluation [23,36]. However, these two techniques are unable to clearly display micro-low-speed blood flow signals or provide quantitative analysis. By contrast, SMI outperforms in assessing micro-low-speed blood flow and providing the VI to realize quantitative assessment. It has been widely used in superficial tissues and organs, achieving great progress in recent years [24].

In a previous study, CD31 was validated as a marker protein expressed on the surface of vascular endothelial cells, which has been widely used to quantify angiogenesis [37]. Therefore, we utilized this index to reflect the density of angiogenesis in HS, further substantiating the validity of SMI. In our study, CD31 expression decreased with increasing BTXA concentration. However, the VI obtained based on SMI showed no significant difference between the groups, possibly due to the following reason. The wounds were so superficial that the use of a pad was required, which caused unavoidable pressure during VI measurements. Consequently, the tissues close to the pad presented interference signals of vascularity. These interference signals were taken into account as blood flow signals in the calculation of VI, which might lead to uncertainty in the measurement. During our evaluation, we tried to draw the ROI

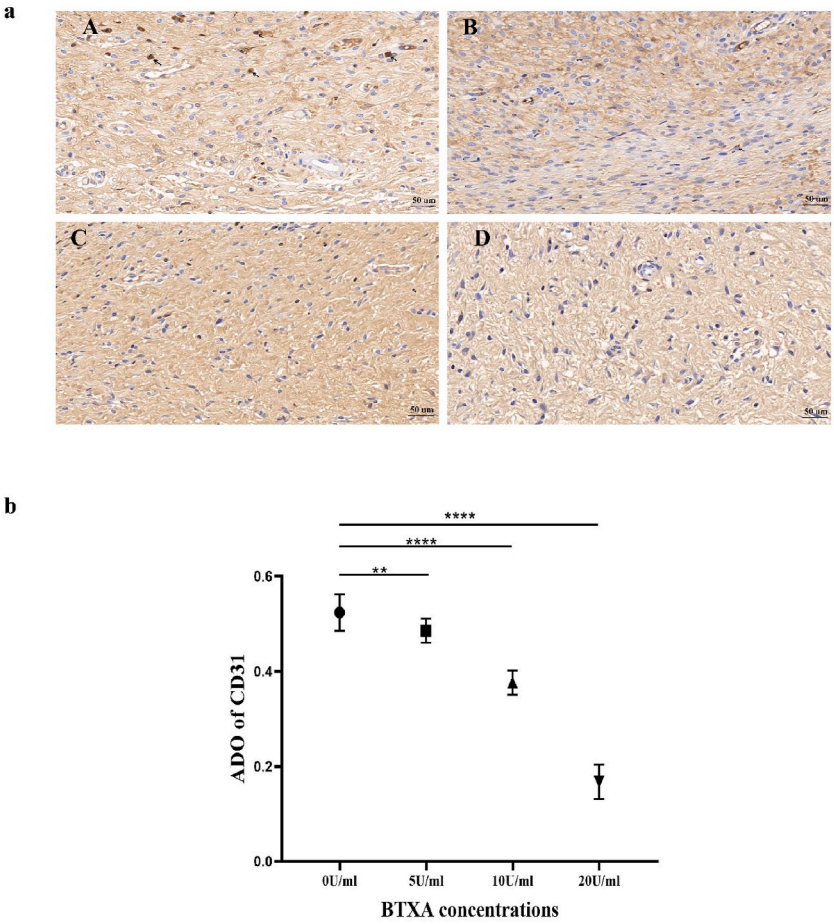

Fig. 7. Angiogenesis evaluation in hypertrophic scars based on CD31 staining. a Images of immunohistochemical staining for CD31 in the different groups. Arrows indicate positively stained vessels. (A) 0 U/ml group, (B) 5 U/ml group, (C) 10 U/ml group, and (D) 20 U/ml group. b Quantitative analysis of CD31 expression in the different groups. Compared with the 0 U/ml group, all differences were statistically significant. (**$p < 0.01$; ****$p < 0.001$).

manually to avoid containing too many non-target areas. But we found it difficult to draw the ROI accurately because the scars were so small. Although the expected results were not achieved, we found that SMI could clearly show the microvascular perfusion in the scar and present microvascular distribution of the lesion area in real time. Therefore, if we could avoid the generation of interference signals, it is possible that the value of VI could be used to evaluate the vascularity of scars quantitatively. In the future study, we will optimize our experimental and measurement methods to verify this possibility.

Scars consist of excess collagen, which leads to increased hardness and diminished elasticity. According to a previous study, improved elasticity is regarded as an objective parameter indicating successful treatment [28]. Elasticity detected by ultrasound is an effective and reliable objective reflection of scar stiffness [36]. SWE is an ultrasound technique for evaluating tissue stiffness. An earlier study indicated that the shear wave velocity measured by SWE in burn scar patients could be used to assess scar severity [25]. Moreover, SWE has been proven to be a useful indicator in predicting keloid activity [36].

In the inflammatory and proliferative stages during scar formation, collagen gradually deposits around the microvessels [38]. BTXA was proven to reduce extracellular matrix synthesis, including collagen [39]. Therefore, monitoring the changes of collagens in HS is beneficial to evaluate the therapeutic effect of BTXA. Masson staining could display the collagen fibrils in scars, but this method is invasive. The excess collagen in scars could lead to increased hardness and diminished elasticity [36]. In our study, the elasticity evaluation image revealed that HSs were harder than normal skin, whereas they became softer with increasing BTXA concentration. Moreover, the collagen expression levels displayed a good correlation with the shear wave velocity measured by SWE, which also demonstrated that the value of shear wave velocity could indirectly reflect the collagen content. In a previous study, DeJong H et al. utilized SWE to measure shear wave velocity of hypertrophic burn scars and found high correlations between the velocity and VSS pliability sub-scores [25]. This is consistent with our findings. In contrast to most previous studies, we validated the accuracy of SWE with Masson staining, and SWE has an advantage over VSS in that VSS mainly relies on the subjective experience of clinicians. This result demonstrated that SWE has a good performance in evaluating the therapeutic effect of BTXA in HS.

VSS is the most commonly used scar assessment method within the clinical area. Compared to the scar thickness evaluation in the

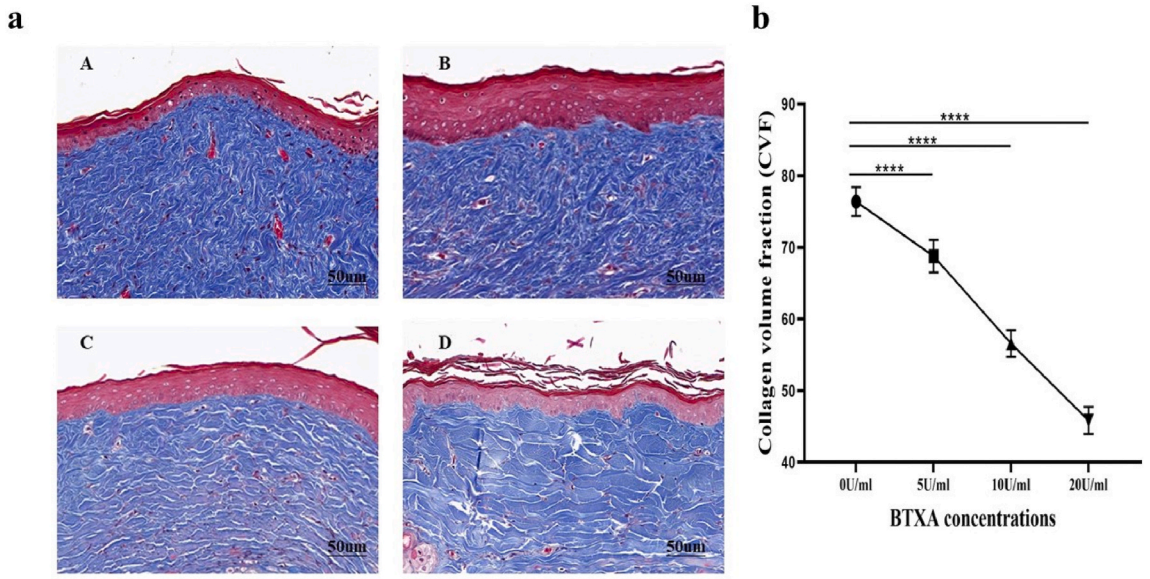

Fig. 8. Botulinum toxin type A inhibited collagen proliferation in a dose-dependent manner. Red color indicates cells and blue color indicates collagen fibrils. a Representative Masson staining images of HSs in the different groups. (A) 0 U/ml group, (B) 5 U/ml group, (C) 10 U/ml group, and (D) 20 U/ml group. b The mean value of the CVF in the different groups. Compared with the 0 U/ml group, all differences were statistically significant ($^{****}p < 0.001$).

scale, the thickness of the scar measured by HFUS can provide a more accurate assessment of the total thickness of the dermis and epidermis of the scar. SWE could assess the hardness of scars quantitatively, that is the flexibility in the VSS, which could quantify the subjective parameters. SMI has shown great potential in the assessment of the intravascular perfusion of scar, which could clearly display the intravascular perfusion of scar. What is more, SMI could provide the vascular index by its own algorithm to evaluate the vessel density quantitatively. These ultrasound techniques have the advantages of convenience, non-invasiveness, and economy, and have great potential in evaluating the curative effect of scar.

This study had several limitations. First, the sample size and the wound size of this study were small, which may have induced avoidable bias. Second, scar evaluations were not conducted at different time intervals. Because pathological sections had to be obtained from every model after evaluation, a time-course would have demanded a large number of rabbit models. Third, other elastography techniques, such as instantaneous elastography, were not utilized for comparative analysis. Lastly, our study did not include a comparison with normal tissue. In future research, the sample size should be increased, and studies should concentrate on more noninvasive quantitative indicators based on ultrasound and investigate whether they have linear relationships or other functional relationships with pathological and immunological analyses. Comparative studies between scar and normal tissue are also recommended to understand whether treatments with different concentrations of BTXA are closer to normal tissue properties or are over-treatments. In addition, we would attempt to establish a multimodal imaging system based on multimodal ultrasound parameters, which may provide better performance.

5. Conclusion

Finding methods that are both noninvasive and objective to evaluate the therapeutic effects on scars is crucial for achieving better management. Our study demonstrated the potential of HFUS, SMI, and SWE in evaluating HS vascularity and stiffness. HFUS and SWE displayed excellent performance in assessing the therapeutic effects of BTXA, and SMI could show microvascular perfusion in HS. These ultrasound techniques have tremendous potential in evaluating therapeutic effects on HS, enabling targeted interventions based on the evaluation. Timely adjustment of treatment based on objective assessments during scar management could reduce the occurrence of both over- and undertreatment. Nonetheless, further studies are still required to obtain more detailed insights.

Ethics statement

This study was reviewed and approved by the Animal Experimentation Ethics Committee of Anhui Medical University, with the approval number: LLSC20221114.

Data availability statement

Data will be made available on request.

CRediT authorship contribution statement

Liu-liu Cao: Writing – original draft. **Zhi-guo Yang:** Data curation. **Wei-hong Qi:** Investigation. **Huan Zhang:** Data curation. **Yu Bi:** Data curation. **Yong Shan:** Data curation. **Xin-wu Cui:** Writing – review & editing. **Fan Jiang:** Writing – review & editing.

Declaration of competing interest

The authors declare that they have no known competing financial interests or personal relationships that could have appeared to influence the work reported in this paper.

Acknowledgements

We thank International Science Editing (http://www.internationalscienceediting.com) for providing language help and writing assistance.

References

[1] Y. Lv, et al., Low-intensity ultrasound combined with 5-aminolevulinic acid administration in the treatment of human tongue squamous carcinoma, Cell. Physiol. Biochem. 30 (2) (2012) 321–333.
[2] C.Y. Demir, et al., Comparison of enalapril, candesartan and intralesional triamcinolone in reducing hypertrophic scar development: an experimental study, Aesthetic Plast. Surg. 42 (2) (2018) 352–361.
[3] P. Martin, R. Nunan, Cellular and molecular mechanisms of repair in acute and chronic wound healing, Br. J. Dermatol. 173 (2) (2015) 370–378.
[4] L. Butzelaar, et al., Going into surgery: risk factors for hypertrophic scarring, Wound Repair Regen. 23 (4) (2015) 531–537.
[5] F.B. Rabello, C.D. Souza, J.A. Farina Júnior, Update on hypertrophic scar treatment, Clinics 69 (8) (2014) 565–573.
[6] M.L. Elsaie, Update on management of keloid and hypertrophic scars: a systemic review, J. Cosmet. Dermatol. 20 (9) (2021) 2729–2738.
[7] V. Vorstandlechner, et al., The secretome of irradiated peripheral mononuclear cells attenuates hypertrophic skin scarring, Pharmaceutics 15 (4) (2023).
[8] F.M. Ghazawi, et al., Insights into the pathophysiology of hypertrophic scars and keloids: how do they differ? Adv. Skin Wound Care 31 (1) (2018) 582–595.
[9] A.J. Robinson, M.F. Khadim, K. Khan, Keloid scars and treatment with botulinum toxin type A: the belfast experience, J. Plast. Reconstr. Aesthetic Surg. 66 (3) (2013) 439–440.
[10] X.G. Liu, D. Zhang, Evaluation of efficacy of corticosteroid and corticosteroid combined with botulinum toxin type A in the treatment of keloid and hypertrophic scars: a meta-analysis, Aesthetic Plast. Surg. 45 (6) (2021) 3037–3044.
[11] T.A. Mustoe, et al., International clinical recommendations on scar management, Plast. Reconstr. Surg. 110 (2) (2002) 560–571.
[12] H. Wang, et al., [The use of glucocorticoid in the management of adverse effects related to immunocheckpoint inhibitors], Zhongguo Fei Ai Za Zhi 22 (10) (2019) 615–620.
[13] L.M. Kasyanju Carrero, et al., Botulinum toxin type A for the treatment and prevention of hypertrophic scars and keloids: updated review, J. Cosmet. Dermatol. 18 (1) (2019) 10–15.
[14] Q.U.A. Javed, et al., Evaluation and optimization of prolonged release mucoadhesive tablets of dexamethasone for wound healing: in vitro-in vivo profiling in healthy volunteers, Pharmaceutics 14 (4) (2022).
[15] J.P. Andrews, et al., Keloids: the paradigm of skin fibrosis - pathomechanisms and treatment, Matrix Biol. 51 (2016) 37–46.
[16] M.H. Viera, A.C. Vivas, B. Berman, Update on keloid management: clinical and basic science advances, Adv. Wound Care 1 (5) (2012) 200–206.
[17] M.G. Yoo, I.H. Kim, Keloids and hypertrophic scars: characteristic vascular structures visualized by using dermoscopy, Ann. Dermatol. 26 (5) (2014) 603–609.
[18] C. Chen, et al., Heterogeneous features of keloids assessed by laser speckle contrast imaging: a cross-sectional study, Laser Surg. Med. 53 (6) (2021) 865–871.
[19] Q. Liu, et al., Increased blood flow in keloids and adjacent skin revealed by laser speckle contrast imaging, Laser Surg. Med. 48 (4) (2016) 360–364.
[20] M. Renaud, et al., Intraoral ultrasonography for periodontal tissue exploration: a review, Diagnostics 13 (3) (2023).
[21] S.Y. Huang, et al., Quantitative assessment of treatment efficacy in keloids using high-frequency ultrasound and shear wave elastography: a preliminary study, Sci. Rep. 10 (1) (2020) 1375.
[22] J. Hang, et al., Correlation between elastic modulus and clinical severity of pathological scars: a cross-sectional study, Sci. Rep. 11 (1) (2021) 23324.
[23] A.M. Elrefaie, R.M. Salem, M.H. Faheem, High-resolution ultrasound for keloids and hypertrophic scar assessment, Laser Med. Sci. 35 (2) (2020) 379–385.
[24] Z. Fu, et al., Clinical applications of superb microvascular imaging in the superficial tissues and organs: a systematic review, Acad. Radiol. 28 (5) (2021) 694–703.
[25] H. DeJong, et al., Objective quantification of burn scar stiffness using shear-wave elastography: initial evidence of validity, Burns 46 (8) (2020) 1787–1798.
[26] R. Guo, et al., Quantitative assessment of keloids using ultrasound shear wave elastography, Ultrasound Med. Biol. 46 (5) (2020) 1169–1178.
[27] Z.G. Kaya İslamoğlu, E. Uysal, A preliminary study on ultrasound techniques applied to cicatricial alopecia, Skin Res. Technol. 25 (6) (2019) 810–814.
[28] K.C. Lee, et al., A systematic review of objective burn scar measurements, Burns Trauma 4 (2016) 14.
[29] D.S. Masson-Meyers, et al., Experimental models and methods for cutaneous wound healing assessment, Int. J. Exp. Pathol. 101 (1–2) (2020) 21–37.
[30] Z. Yang, et al., Concentration-dependent inhibition of hypertrophic scar formation by botulinum toxin type A in a rabbit ear model, Aesthetic Plast. Surg. 46 (6) (2022) 3072–3079.
[31] N.A. Agabalyan, et al., Comparison between high-frequency ultrasonography and histological assessment reveals weak correlation for measurements of scar tissue thickness, Burns 43 (3) (2017) 531–538.
[32] L. Forbes-Duchart, et al., Burn therapists' opinion on the application and essential characteristics of a burn scar outcome measure, J. Burn Care Res. 30 (5) (2009) 792–800.
[33] M. Simons, Z. Tyack, Health professionals' and consumers' opinion: what is considered important when rating burn scars from photographs? J. Burn Care Res. 32 (2) (2011) 275–285.
[34] E.H. Dutra, et al., Cellular and matrix response of the mandibular condylar cartilage to botulinum toxin, PLoS One 11 (10) (2016) e0164599.
[35] N. Kurokawa, K. Ueda, M. Tsuji, Study of microvascular structure in keloid and hypertrophic scars: density of microvessels and the efficacy of three-dimensional vascular imaging, J Plast Surg Hand Surg 44 (6) (2010) 272–277.
[36] C. Chen, et al., Activity of keloids evaluated by multimodal photoacoustic/ultrasonic imaging system, Photoacoustics 24 (2021) 100302.
[37] Y. Song, et al., Usnic acid inhibits hypertrophic scarring in a rabbit ear model by suppressing scar tissue angiogenesis, Biomed. Pharmacother. 108 (2018) 524–530.
[38] Q. Chun, et al., Dynamic biological changes in fibroblasts during hypertrophic scar formation and regression, Int. Wound J. 13 (2) (2016) 257–262.
[39] Z. Xiao, G. Qu, Effects of botulinum toxin type a on collagen deposition in hypertrophic scars, Molecules 17 (2) (2012) 2169–2177.